

Evaporative Cooling in Semiconductor Devices

Thushari Jayasekera, Kieran Mullen, and Michael A. Morrison*
*Department of Physics and Astronomy, The University of Oklahoma,
440 West Brooks Street, Norman, Oklahoma 73019-0225*

We discuss the theory of cooling electrons in solid-state devices via “evaporative emission.” Our model is based on filtering electron subbands in a quantum-wire device. When incident electrons in a higher-energy subband scatter out of the initial electron distribution, the system equilibrates to a different chemical potential and temperature than those of the incident electron distribution. We show that this re-equilibration can cause considerable cooling of the system. We discuss how the device geometry affects the final electron temperatures, and consider factors relevant to possible experiments. We demonstrate that one can therefore substantial electron cooling due to quantum effects in a room-temperature device. The resulting cooled electron population could be used for photo-detection of optical frequencies corresponding to thermal energies near room temperature.

PACS numbers: 73.50.Lw, 73.23.-b

I. INTRODUCTION

As electronic devices become smaller, they leave the regime of classical physics and enter the realm of quantum physics. Many classical quantities such as resistance must be reinterpreted for systems on a mesoscopic scale. One such classical concept is that of the refrigerator: a device that uses an external source of work to cool a gas. In this paper we consider whether this classical concept can be applied to an electron gas so that one could cool such a gas by applying a voltage to a device.

There are many ways to cool electrons in a condensed-matter system. For example, thermoelectric coolers based on the Peltier effect¹ are available commercially. A different kind of electron-cooling mechanism in semiconductor devices is based on a quasistatic expansion of a two-dimensional electron gas.² Still other possibilities include taking advantage of many-body effects that can lead to liquid/gas phase transitions in the electron population in a semiconductor quantum well.^{3,4}

In this paper we investigate electron cooling in a mesoscopic solid-state device using evaporative emission. This method entails removal of (“filtering”) electrons from a high-energy subband of a many-electron system, followed by relaxation of the remaining electrons to a temperature lower than that of the initial system. Evaporative cooling is widely used in bosonic systems.⁵ But this method is harder to implement for fermionic systems, as we shall discuss below.

In section II we describe the theory of a two-dimensional device to cool electrons in quantum wires. We use the Landauer formula^{6,7,8} to analyze the cooling properties of these devices. This formula was originally developed to explain the transport properties of electrons in a quantum device. It relates these properties to the quantum mechanical scattering amplitudes for electrons that pass through the device. To calculate these amplitudes, we use an extension of R-matrix theory^{9,10,11} that we summarize in the Appendix. In section III we use this theory to calculate cooling properties of several two-dimensional devices. We begin with a simple T-junction

device and show that by optimizing its design we can achieve electron cooling. We improve upon this result by switching to a “plus-junction” design, which can give up to 15% cooling. In section IV we discuss applications and realistic parameters for a device to cool electrons, and in V we summarize our key results and describe future research.

II. ELECTRON COOLING IN TWO-DIMENSIONAL QUANTUM DEVICES

Our theoretical approach is analogous to the working principle of the classical Hilsch vortex tube,¹³ which uses a T-shaped assembly of pipes to separate high-pressure air into a high-temperature system and a low-temperature system. This separation does not violate the Second Law of Thermodynamics, because the system is driven by an external force.

We use a similar idea to cool electrons in a quantum mechanical system. The simplest such device uses a T-shaped assembly of quantum wires to remove higher-energy electrons from an electron gas at fixed temperature. Figure 1 is a schematic of such a configuration that defines the regions of the device. We assume that our device is formed from a quantum well whose thickness is sufficiently small that the device can be considered two-dimensional. That is, we assume that the device confines electrons to a layer of thickness z_0 such that the confinement energy associated with motion in the z -direction is much larger than any other energy in the problem. (This confinement energy is $\hbar^2\pi^2/2m^*z_0^2$, where m^* is the electron effective mass.)

There are three leads in the T-junction: the input lead, output lead, and sidearm, as shown in Fig.1. We shall label physical quantities by subscripts “i,” “o,” and “s” respectively; for example, we denote the widths of the leads by w_i , w_o , and w_s . Electrons are injected into this device through the input lead, and in the input region are in thermal equilibrium at an initial temperature T_i and chemical potential μ_i . Filtering of higher-energy elec-

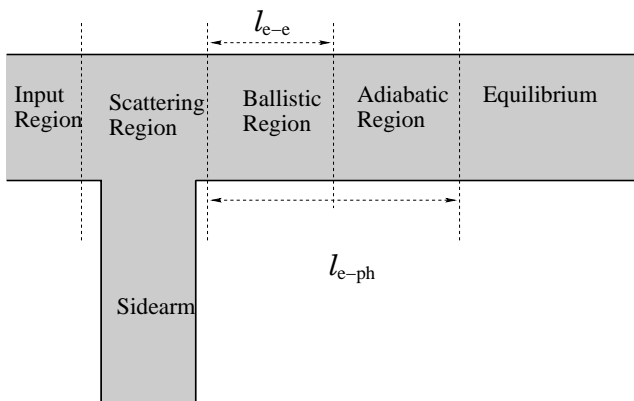


FIG. 1: Regions in a two-dimensional T-junction device. The “ballistic region” is the part of the device within a distance comparable to the electron-electron scattering length (l_{e-e}) of the junction. The “adiabatic region” is within the electron-phonon scattering length (l_{e-ph}) of the junction. It is in the adiabatic region that we achieve cooling. At larger distances, in the “equilibrium region,” the electrons have returned to the temperature of the lattice.

trons from the initial electron gas occurs in the *scattering region*. The rate of scattering into the sidearm depends upon the electron energy: if the subband energy in lead of width w is given by $E_n = \hbar^2 \pi^2 n^2 / 2mw^2$, then the “force” electrons exert on the sides of the lead, $F = -dE/dw$, is larger for larger n . Thus when an electron encounters the sidearm, the higher-subband states are more likely to squirt down the sidearm. Alternatively, one can see that the higher-subband electrons scatter preferentially to the sidearm because they are in states with wave functions that are linear combinations of plane waves with larger transverse momenta.

Electrons that scatter forward into the output lead proceed into the *ballistic region*, where the electron population is determined entirely by the product of the initial electron distribution and the scattering probability. Next the electrons enter the *adiabatic region*, where they exchange energy among themselves and so relax to a temperature T_o and a chemical potential μ_o . In principle, the values of these properties can be calculated from conservation laws for energy and particle number. In section III we report such calculations and show that for some device geometries the temperature T_o is less than the initial temperature: *this temperature decrease is the desired cooling effect*.

Finally, at large distances (as determined by the electron-phonon scattering rate) the electrons will return to equilibrium with the lattice at the initial temperature T_i ; this re-equilibration occurs in the *equilibrium region*. To see cooling, one must measure the electron temperature before they get to this region

Below we define our notation and describe how we calculate the electron distributions in the input and output leads. We also define and describe the calculation of a quantitative measure of electron cooling in the device.

A. Input electron densities and populations

Provided the electrons in each lead are in thermodynamic equilibrium, we can treat them as an ideal Fermi gas. For lead ℓ , therefore, the subband electron density (per unit volume) in an open (energetically accessible) subband n is

$$\rho_n^{(\ell)}(E, T_\ell, \mu_\ell) = f(E; T_\ell, \mu_\ell) \mathcal{D}_n^{(\ell)}(E) \quad (1)$$

for n such that the subband energy obeys $\epsilon_n^{(\ell)} \leq E$. In this equation, the density of states is

$$\mathcal{D}_n^{(\ell)}(E) = [E - \epsilon_n^{(\ell)}]^{-1/2}. \quad (2)$$

The quantity E is the dimensionless electron energy measured in units of the lowest subband energy of the input channel, $\mathcal{E}_1^i \equiv \hbar^2 \pi^2 / 2m^* w_i^2$. We choose the zero of energy at the energy of the ground transverse state in the input lead. We measure all other subband thresholds relative to this energy and in units of \mathcal{E}_1^i , so that

$$\epsilon_n^{(\ell)} = n^2 \frac{w_i^2}{w_\ell^2} - 1. \quad (3)$$

The occupation probability for lead ℓ is given by the Fermi-Dirac distribution function for total electron energy $E = E_n^{(\ell)} + \epsilon_n^{(\ell)}$,

$$f(E; T, \mu_\ell) = \frac{1}{e^{(E - \mu_\ell)/k_B T} + 1}, \quad (4)$$

where μ_ℓ is the electrochemical potential in lead ℓ , $E_n^{(\ell)}$ is the *longitudinal kinetic energy* of the electron, and k_B is Boltzmann’s constant. The corresponding subband population in lead ℓ is the integral of the subband density (Eq. (1)) over all allowed total electron energies E :

$$N_n^{(\ell)}(T_\ell, \mu_\ell) = \int_{\epsilon_n^{(\ell)}}^{\infty} \rho_n^{(\ell)}(E; T_\ell, \mu_\ell) dE. \quad (5)$$

The total population in lead ℓ is the sum of the subband populations for that lead,

$$N^{(\ell)}(T_\ell, \mu_\ell) = \sum_{n=1}^{\infty} N_n^{(\ell)}(T_\ell, \mu_\ell). \quad (6)$$

B. Transmitted-electron densities and populations

Immediately upon leaving the scattering region the transmitted electrons are in a highly nonequilibrium distribution and cannot be characterized by a temperature or a chemical potential. By the time these electrons have traveled a distance along the lead comparable to several times their relaxation length, they have come to equilibrium at T_o and μ_o , and it is meaningful to describe

them by a Fermi-Dirac distribution function $f(E; T_o, \mu_o)$. These output-lead properties refer to the electron population in the adiabatic region, where the electrons are in thermodynamic equilibrium. Given T_i and μ_i for the *input* lead, our goal is to determine the values of T_o and μ_o for the *output* lead that yields the lowest $T_o < T_i$; i.e., which maximizes cooling of transmitted electrons.

For a given T_i and μ_i , we can determine the temperature in the output lead T_o by requiring that the number of electrons in the output lead at equilibrium equals the number of electrons transmitted into this lead (conservation of electrons in the output lead). To set up equations to implement this strategy, we must define subband and lead populations in terms of electrons transmitted from the input lead into the output lead. The (state-to-state) density of electrons transmitted from an open subband n of the input lead i into an open subband n' of a lead ℓ' is

$$\rho_{n',n}^{\ell',i}(E; T_i, \mu_i) = \rho_n^{(i)}(E, T_i, \mu_i) \mathcal{T}_{n',n}^{\ell',i} \quad (7)$$

for $E \geq \epsilon_{n',n}^{\max}$, where $\mathcal{T}_{n',n}^{\ell',i}$ is the transmission coefficient from subband n in lead i to subband n' in lead ℓ' . The restriction that the total electron energy E be greater than or equal to

$$\epsilon_{n',n}^{\max} \equiv \max \left\{ \epsilon_n^{(i)}, \epsilon_{n'}^{(\ell')} \right\} \quad (8)$$

ensures that subbands n and n' are both open; were this restriction violated, then the transmission coefficient $\mathcal{T}_{n',n}^{\ell',i}$ would be undefined.

The population of electrons transmitted into subband n' of the output lead, the transmitted subband density, is

$$N_{n'}^{o,i}(T_i, \mu_i) = \sum_{n=1}^{\infty} \int_{\epsilon_{n',n}^{\max}}^{\infty} \rho_{n',n}^{o,i}(E; T_i, \mu_i) dE. \quad (9)$$

Hence the total population of electrons transmitted into the output lead, the transmitted density, is

$$N_{n'}^{o,i}(T_i, \mu_i) = \sum_{n'=1}^{\infty} N_{n'}^{o,i}(T_i, \mu_i). \quad (10)$$

C. The cooling parameter

For a given T_i and μ_i , we can determine the equilibrium temperature in the output lead T_o by solving simultaneously the equation for conservation of the number of electrons,

$$N^{(o)}(T_o, \mu_o) = N^{o,i}(T_i, \mu_i), \quad (11)$$

and the equation for conservation of electron energy in this lead:

$$\langle E \rangle^{(o)}(T_o, \mu_o) = \langle E \rangle^{o,i}(T_i, \mu_i). \quad (12)$$

In Eq. (12) the energy of the electrons at equilibrium in the output lead is

$$\langle E \rangle^{(o)}(T_o, \mu_o) \equiv \sum_{n'=1}^{\infty} \int_{\epsilon_{n'}^{(o)}}^{\infty} E \rho_{n'}^{(o)}(E; T_o, \mu_o) dE, \quad (13)$$

where the subband density in the output lead, $\rho_{n'}^{(o)}(E; T_o, \mu_o)$ is defined by Eq. (1). The energy of the electrons *transmitted into the output lead* is

$$\langle E \rangle^{o,i}(T_i, \mu_i) = \sum_{n'=1}^{\infty} \sum_{n=1}^{\infty} \int_{\epsilon_{n',n}^{\max}}^{\infty} E \rho_{n',n}^{o,i}(E; T_i, \mu_i) dE, \quad (14)$$

where the transmitted-electron density $\rho_{n',n}^{o,i}(E; T_i, \mu_i)$ is given by Eq. (7). Using Eqs. (10), and (14) we calculate the number of transmitted electrons and their energy. We then calculate the equilibrium temperature and chemical potential that would give the same total number and energy. This calculation produces the parameters T_o and μ_o for the output lead.

As a measure of the effectiveness of a given device for cooling electrons, we define the cooling parameter

$$\eta(T_i, \mu_i) \equiv \frac{T_o(T_i, \mu_i)}{T_i}. \quad (15)$$

If $\eta > 1$, the device *heats* electrons. Our goal, therefore, is to determine the device geometry and initial electron properties T_i and μ_i that minimize $\eta < 1$.

III. RESULTS

To achieve optimum cooling the higher-subband electrons should scatter into the sidearm, and the lower-subband electrons should scatter into the output lead. In a real device not all higher-subband electrons will scatter into the sidearm, and not all the lower-subband electrons will scatter into the output lead. The probabilities for electron scattering, as quantified in transmission coefficients, depend on system properties such as the geometry, and on scattering potentials. We consider “perfect devices” that have no impurities, so electrons are scattered only by the boundaries of the device. We further assume that the potential energy of the electrons in the leads is zero; this simplifying assumption is *not* essential to either the cooling effect or to our formalism. We can alter the scattering of electrons by changing the ratio of the width of the sidearm to that of the input lead (Fig. 1) or by changing the geometry altogether.

A. T-junction cooling devices

To calculate the cooling parameter η we need to know the population of electrons in each subband. To determine this quantity we must know transmission coefficients from a state in the input lead to states in the output lead. To calculate these transmission coefficients we use a generalization of R-matrix theory that we summarize in the Appendix. To determine the results reported here, we calculated cooling parameters η using transmission coefficients in a T-junction device for various ratios of the width w_s of the sidearm to the width w_i of the input lead, keeping the width w_o of the output lead equal to w_i .

1. A T-junction device with $w_s = w_i = 1.0$

We first consider a T-junction device in which all leads have the same width: $w_i = w_s = w_o$. Figure 2(a) shows “state-to-lead” transmission coefficients for scattering into the output lead of electrons in different subbands of the input lead. These coefficients are sums over all energetically accessible (“open”) subbands n_o of the output lead of state-to-state transmission coefficients $\mathcal{T}_{n_o, n_i}^{\ell, i}$ [see Eq. 7] from a given state n_i of the input lead. This figure illustrates the loss of some higher-subband electrons from the initial electron distribution.

The cooling parameter η for this case is shown in Fig. 2(b) for different values of initial temperature T_i with the initial chemical potential $\mu_i = 0$. (Note that we measure the energy in terms of \mathcal{E}_1^i , and all the energies are measured from \mathcal{E}_1^i . So $\mu_i = 0$ means that the external potential of the system is such that the Fermi energy is $E_F = \hbar^2 \pi^2 / 2m^* w_i^2$.) For this geometry $\eta > 1$ for all initial temperatures the cooling parameter. That is, this device *heats* electrons—the opposite of the desired effect.

This case is important because it demonstrates that even if high-energy electrons are lost due to scattering, a compensatory loss of low-energy electrons may produce an overall heating effect. Loss of low-energy electrons opens gaps in the electron distribution at low energies. Higher-energy electrons can then relax into these newly accessible low-energy states, with the resulting energy difference liberated as thermal energy. If this happens, then the loss of low-energy electrons will *heat* the system. Even a small dip in the scattered-electron distribution at low energies will significantly affect the final temperature. To *cool* electrons, therefore, it is not sufficient to merely scatter higher-energy electrons. We must scatter thermally excited electrons *but not significantly scatter electrons in lower-energy subbands*.

2. Alternative T-junction geometries

To determine whether a T-junction device can cool electrons, we now consider several widths w_s of the

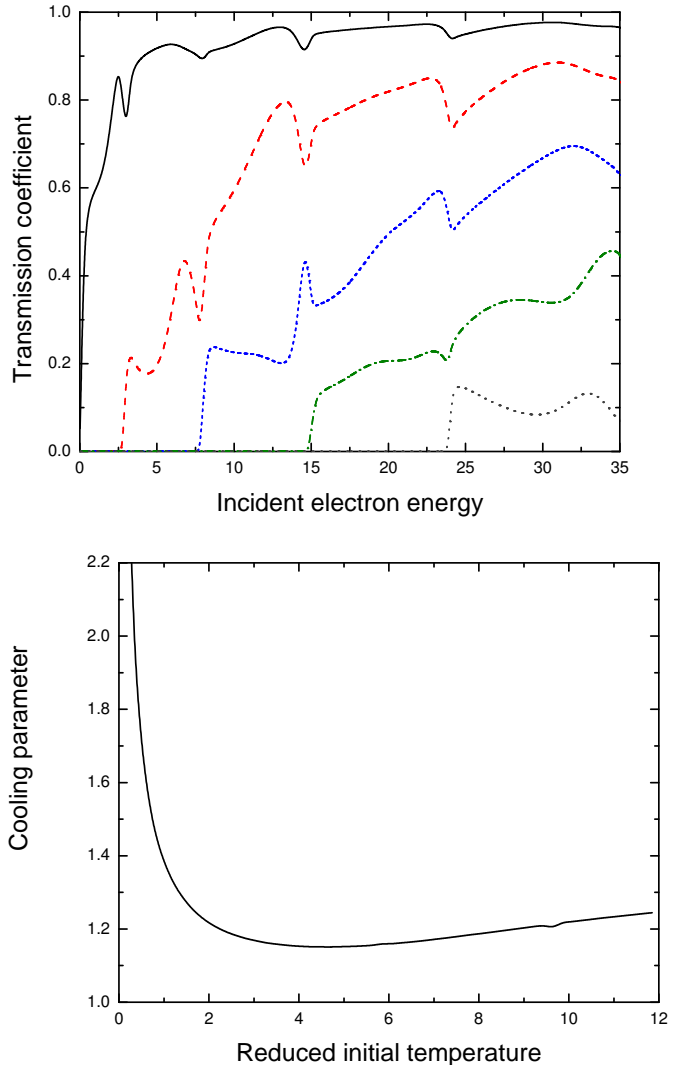


FIG. 2: Upper panel: State-to-output-lead transmission coefficients for electrons in a T-junction device with $w_i = w_s = w_o$. The curves correspond to different subbands of the incident electrons: $n_i = 1$ (solid curve), 2 (dashed), 3 (short dash), 4 (dash-dot), 5 (dotted). The horizontal axis is the energy of the incoming electron measured in terms of the first-subband energy of the input lead, $\mathcal{E}_1^i = \hbar^2 \pi^2 / 2m^* w_i^2$, from a zero of energy at \mathcal{E}_1^i . Lower panel: The cooling parameter η for the coefficients in (a) for initial chemical potential $\mu_i = 0$. The “reduced initial temperature” (horizontal axis) is the dimensionless quantity $k_B T_i / \mathcal{E}_1^i$.

sidearm in Fig. 1. For each geometry we determine the initial temperature T_i and chemical potential μ_i that *minimize* the cooling parameter η . Table I shows these data and the corresponding final temperature T_o and chemical potential μ_o for maximum cooling.

To illustrate these data and the effect changing the geometry in this way, we show in Fig 3 the variation of η

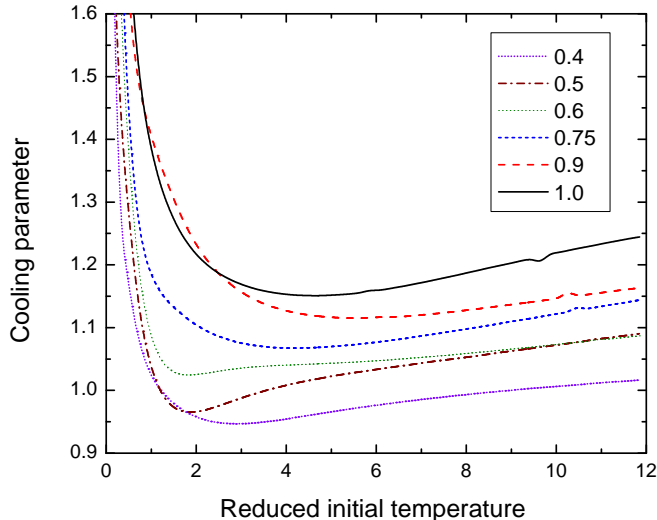


FIG. 3: The cooling parameter η as a function of the reduced initial temperature with initial chemical potential $\mu_i = 0$ for different values of w_s/w_i . The cooling parameter decreases with increasing magnitude of $w_s/w_i = 1.0$ (solid line), 0.9 (long dash), 0.75 (medium dash), 0.6 (short dash), 0.5 (dash-dot), and 0.4 (dotted). The reduced initial temperature is defined in the caption to Fig. 2.

w_s	μ_i	T_i	T_o	μ_o	η
1.0	0.0	4.65	5.35	-6.24	1.15
	3.0	5.85	7.06	-5.63	1.21
	6.0	6.77	8.69	-5.06	1.28
0.9	0.0	5.68	6.34	-6.27	1.11
	3.0	6.52	7.58	-4.97	1.16
	6.0	7.63	9.33	-4.31	1.22
0.75	0.0	4.18	4.463	-3.68	1.07
	3.0	5.36	6.01	-2.58	1.22
	6.0	6.59	7.84	-1.80	1.19
0.6	0.0	1.79	1.84	-1.09	1.02
	3.0	6.00	6.53	-1.84	1.09
	6.0	7.39	8.40	-0.77	1.14
0.5	0.0	1.85	1.79	-0.75	0.96
	3.0	3.62	3.86	0.38	1.06
	6.0	6.52	7.35	0.58	1.13
0.4	0.0	2.89	2.73	-0.71	0.95
	3.0	3.28	3.25	1.54	0.99
	6.0	5.47	5.74	2.75	1.05

TABLE I: Cooling parameters η of T-junctions with different sidearm widths w_s . Also shown are the input chemical potential μ_i , output chemical potential μ_o , and output temperature T_o for maximum cooling.

with initial temperature T_i (for initial chemical potential $\mu_i = 0$) for different sidearm widths. These results show that we achieve cooling ($\eta < 1$) for some geometries and

heating ($\eta > 1$) for others. Only the transmission coefficients depend on the device geometry, so it is through these quantum-mechanical scattering probabilities that we can control the extent to which a device can cool electrons.

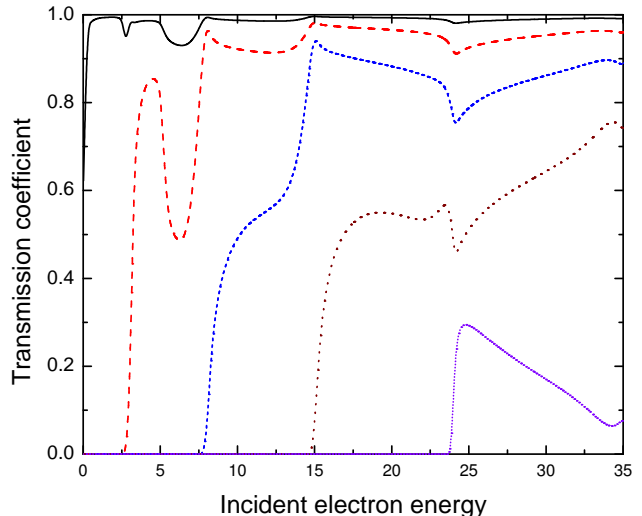


FIG. 4: State-to-lead transmission coefficients for electrons in a T-junction device with $w_i = w_o$ and $w_s = 0.4w_i$. Electron are scattered into the output lead from subbands of the input lead $n_i = 1$ (solid curve), 2 (long dash), 3 (medium dash) 4 (short dash), and 5 (dotted). The horizontal axis is the energy of the incoming electron measured in terms of the first-subband energy of the input lead, $\mathcal{E}_1^i = \hbar^2\pi^2/2m^*w_i^2$, from a zero of energy at \mathcal{E}_1^i . See also the data in Tbl. I, which analyzes cooling for this case.

We shall now consider in detail a device with $w_s/w_i = 0.4$, which gives $\sim 0.05\%$ cooling. Figure 4 shows state-to-lead transmission coefficients for such a device. Different curves correspond to different initial subbands. At low energies the transmission probability is nearly unity, so for this geometry no low-energy electrons are lost from the initial distribution. Were we to adjust the Fermi energy of this device so only the lowest two subbands were occupied, we would see cooling.

In Fig. 5 we illustrate the dependence of the cooling effect on the initial chemical potential μ_i . This figure shows the cooling parameter η for $w_s/w_i = 0.4$ as a function of the initial temperature T_i for $\mu_i = 0.0, 3.0$, and 6.0 . Electron cooling is maximized for $\mu_i = 0$, the edge of the lowest subband. At this chemical potential all electrons scattered into the sidearm are in the thermally active region of the Fermi distribution. Cooling is also obtained for $\mu_i = 3.0$, the edge of the second subband. But at larger values of μ_i the device heats electrons.

This example shows that a T-junction *can* cool electrons. We would prefer, however, a device that produces more cooling than 0.05%. Investigation of other

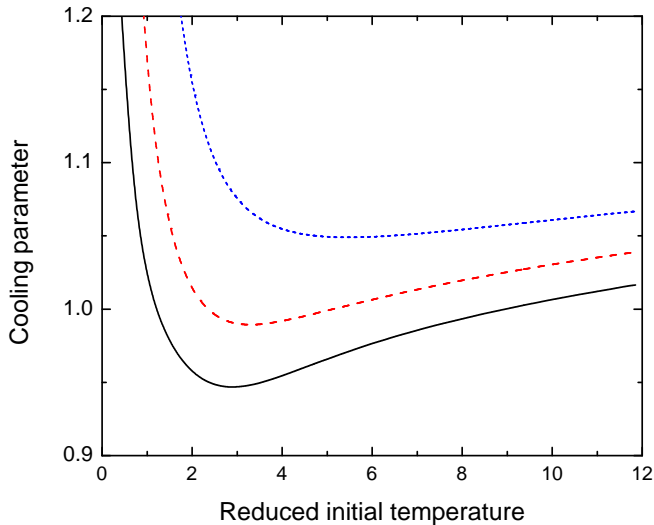


FIG. 5: The cooling parameter η as a function of the reduced initial temperature for a T-junction device with $w_i = w_o$ and $w_s = 0.4w_o$ for three initial chemical potentials, $\mu_i = 0.0$ (solid curve), 3.0 (dashed), and 6.0 (dotted). These data are based on the transmission coefficients shown in Fig. 4. Maximum cooling is obtained for $\mu_i = 0$. The reduced initial temperature is defined in the caption to Fig. 2.

T-junction geometries showed that such a device cannot produce significantly more cooling for any value of w_s/w_i . So we next investigate the addition of a second sidearm. This change produces the “plus junction” illustrated in Fig. 6.

B. A “plus-junction” cooling device

Since we achieved cooling in a T-junction device with $w_s = 0.4$, we shall consider a plus junction with the same lead ratios: $w_i = w_o$ and $w_s/w_o = 0.4$. (Note that the widths of the two sidearms in Fig. 6 are the same.) State-to-lead transmission coefficients for this device are shown in Fig. 7(a), and the resulting cooling parameter η as a function of initial temperature T_i in Fig. 7(b). The latter figure shows that this geometry yields appreciably more electron cooling—greater than 15%—than did the T-junction devices of Tbl. I. A single unit of a plus-junction device with this geometry would cool room-temperature electrons by about $\Delta T = -45C$. Cooling could be further enhanced by combining several such units in sequence. Comparison of this plus-junction to the T-junctions discussion previously, as illustrated in Fig. 8, show how greatly adding a sidearm improves the effectiveness with which this simple device cools electrons.

One could try to further optimize the geometry of

this device by, for example, increasing the width of the sidearms with increasing distance from the junction. Alternatively, one could round the sharp corners at each junction into smooth curves. However, our initial explorations of such alterations (for a T-junction) did not produce substantially more cooling than we obtained with the far simpler plus junction in Fig. 6. The essential features that makes the plus junction more effective than any T junction is the presence of more than one sidearm. It is also essential the threshold for scattering into these sidearms lie above the threshold for the second subband of the input lead.

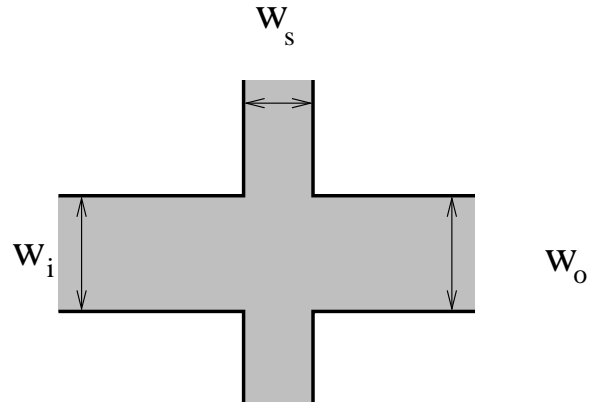


FIG. 6: Schematic of a plus-junction. Note that while the widths of the input and output leads are equal ($w_i = w_o$), the width w_s of the two sidearms may be smaller or larger than w_i . This geometry gives substantially more cooling than any device we have explored that has only a single sidearm.

IV. EXPERIMENTAL CONSIDERATIONS

We now consider a plus-junction device using realistic experimental parameters for Insb and GaAs. While in Sec. III we reported results in dimensionless units, we here use dimensional units.

All material properties depend on the Fermi energy E_F of the system. This quantity is inversely proportional to the effective mass m^* of the electrons in the material and is determined by the electron density in the reservoir. For our device we chose for the initial chemical potential (which is approximately equal to the Fermi energy) $\mu_i = 0$. Since we have scaled the energy by \mathcal{E}_1^i and chosen \mathcal{E}_1^i as the zero of energy, setting the initial chemical potential equals zero means that

$$\mu_i = E_F = \frac{\hbar^2 \pi^2}{2m^* w_i^2}, \quad (16)$$

where w_i is the width of the input lead of the device in Fig. 6. The condition (16) allows us to determine the width of the quantum wire as a function of electron density. Since the Fermi energy and the subband energies

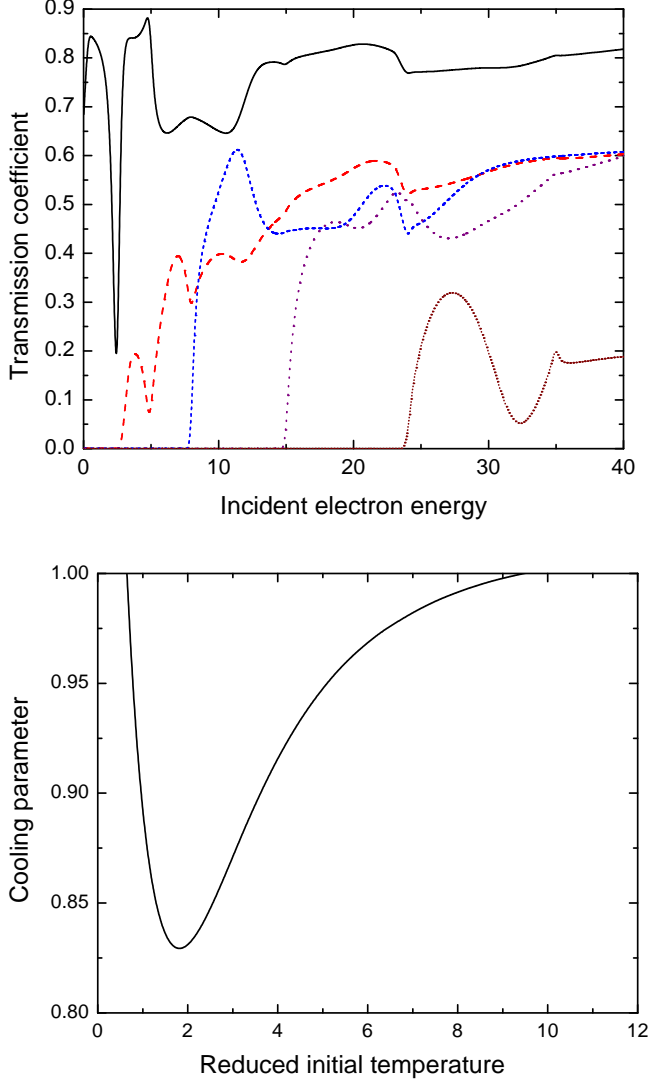


FIG. 7: Upper panel: state-to-output-lead transmission coefficients for electrons in a plus-junction device with $w_s = 0.4w_i$. The curves correspond to different subbands of the incident electrons: $n_i = 1$ (solid curve), 2 (dashed), 3 (short dash), 4 (dash-dot), 5 (dotted). The horizontal axis is the energy of the incoming electron measured in terms of the first-subband energy of the input lead, $\mathcal{E}_1^i = \hbar^2 \pi^2 / 2m^* w_i^2$, from a zero of energy at \mathcal{E}_1^i . Lower panel: Cooling parameter η based on the coefficients shown in the upper panel. The reduced initial temperature is defined in the caption to Fig. 2.

depend on the effective mass in the same fashion, the width of the quantum wire is independent of the material. For a sample with electron density n , we have

$$\frac{\pi \hbar^2}{m^*} n = \frac{\hbar^2 \pi^2}{2m^* w_i^2}, \quad (17)$$

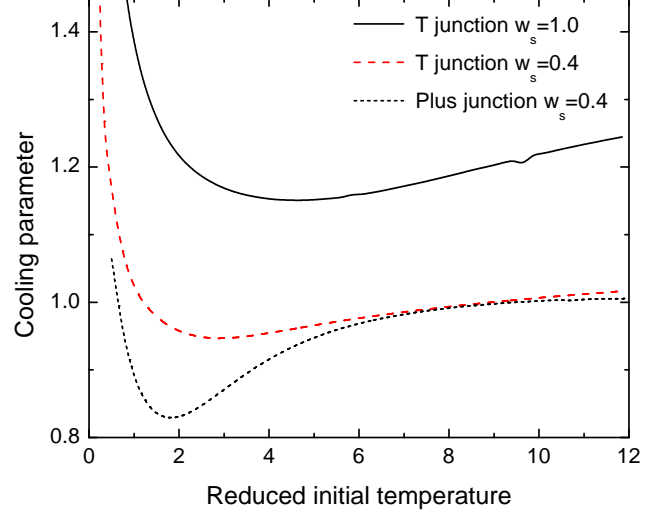


FIG. 8: Cooling parameters for a T-junction with $w_i = w_s = w_o$ (solid line), a T-junction with $w_i = w_o$ and $w_s/w_o = 0.4$ (dashed), and a plus-junction with $w_i = w_o$ and $w_s = 0.4w_i$ (short dash). In all cases the initial chemical potential is $\mu_i = 0$. The reduced initial temperature is defined in the caption to Fig. 2.

which gives for the width of our quantum wire

$$w_i = \sqrt{\frac{\pi}{2n}}. \quad (18)$$

If, for example, $n = 1.0 \times 10^{11} \text{ cm}^{-2}$, we obtain $w_i = 39.6 \text{ nm}$, quite a small value. We can increase this value by decreasing the electron density.

For a plus-junction, we were able to maximize cooling by setting the initial temperature to $T_i \sim 2$ in dimensionless units. In dimensional units, this optimum temperature is

$$k_B T = T_{\text{opt}} \mathcal{E}_1^i, \quad (19a)$$

Using Eq. (16), we obtain

$$k_B T = T_{\text{opt}} E_F. \quad (19b)$$

For a sample with $n = 1.0 \times 10^{11} \text{ cm}^{-2}$, the initial temperature for maximum cooling is $T_i \sim 82 \text{ K}$ for GaAs and $T_i \sim 399 \text{ K}$ for InSb. Room temperature (300K) corresponds to $T \sim 1.5$ for InSb. *One can therefore obtain substantial cooling due to quantum effects in a room-temperature device.* A cooling parameter of $\eta \sim 0.9$ implies that the electron population is cooled by 30K. The resulting cooled electrons could be used for photo-detection of optical frequencies corresponding to thermal energies near room temperature.

The devices we have considered have only one cooling

stage. One could increase cooling by connecting multiple plus junctions in series. The spacing between junctions, however, must be large enough that resonances in scattering between sidearms are negligible. If not, one would have to treat the device as a single large quantum mechanical scattering target. While the presence of such resonances would not preclude cooling, it would make calculations for a chain of junction devices more difficult and sensitive to details of phase breaking.

V. CONCLUSIONS AND PROSPECTS FOR FUTURE RESEARCH

Many photo-detection applications require a cold detector. We have presented results for a prototype device that demonstrates electron cooling in a single-particle picture. We have shown that, while a naive T-junction can produce modest cooling and may produce heating, adding an additional sidearm yields a device that can produce appreciable cooling—at least 15%. The abrupt discontinuities in the confining potentials in these models are not essential to cooling; what is essential is that higher-subband states, which consist of states with larger transverse momenta, scatter appreciable into the sidearms. We therefore expect electron cooling in such devices to be insensitive to details of the potential so long as the potential does not eliminate the states of the lowest subband.

Acknowledgments

This project was supported in part by the US National Science Foundation under Grant MRSEC DMR-0080054, and EPS-9720651, and PHY-0071031. One of the authors (TJ) would like to acknowledge the University of Oklahoma, Graduate College for travel and research grants.

APPENDIX A: R-MATRIX THEORY FOR A 2-D SYSTEM

We consider the two-dimensional system in Fig. 9. This system has a central region A connected to N external regions or “leads.” The leads and the interior region meet at a set of boundary surfaces we denote by S_0, S_1, \dots, S_N . We treat the boundaries between the shaded and unshaded regions as “hard walls” (infinite potential) so electron wave functions are non-zero only in the shaded regions. Since there may be more than three leads, we depart from the notation used in the body of this paper (in which the input, output and sidearm leads were denoted by subscripts i, o , and s) and denote the input lead by a zero subscript and all other leads by positive integer subscripts. We measure all distances in units of w_0 and energies in terms of $E_0 \equiv \hbar^2/2m^* w_0^2$. We seek

an analytic solution for the amplitudes of outgoing states in the leads when only one incoming state is occupied.

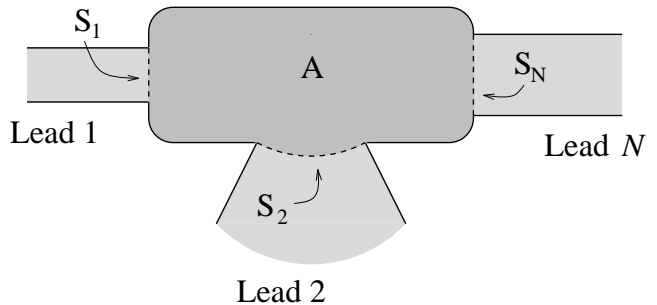


FIG. 9: Schematic of a two-dimensional device for the present scattering calculations. The surfaces S_1, S_2, \dots, S_N separate the interior region A from the N leads.

The time-independent Schrodinger equation for the scattering function is

$$(\hat{H} - E) |\Psi_{E,n_0}\rangle = 0. \quad (\text{A1})$$

where $|\Psi_{E,n_0}\rangle$ represents the state of an electron with kinetic energy E incident in input-lead subband n_0 . Note that $|\Psi_{E,n_0}\rangle$ is well-defined in all leads. In a *finite* region, the Hamiltonian \hat{H} is not Hermitian. We can produce a Hermitian operator by adding to \hat{H} the so-called Bloch operator \hat{L}_B .¹⁰ We denote the eigenfunctions of the sum of these operators in the interior region by $|\phi_i\rangle$ and write the so-called Bloch eigenvalue equation as

$$(\hat{H} + \hat{L}_B) |\phi_i\rangle = E_i |\phi_i\rangle. \quad (\text{A2})$$

Inserting the Bloch operator into the Schrodinger equation we get

$$(\hat{H} + \hat{L}_B - E) \Psi_E = \hat{L}_B \Psi_E. \quad (\text{A3})$$

We now expand the scattering wave function $|\Psi_E\rangle$ in the set of orthonormal Bloch eigenfunctions

$$|\Psi_E\rangle = \sum_j C_j |\phi_j\rangle. \quad (\text{A4})$$

Inserting this expansion into the Schrodinger equation and using the properties of the Bloch eigenfunctions yields

$$|\Psi_{E,n_0}\rangle = \sum_j \frac{\langle \phi_j | \hat{L}_B | \Psi_{E,n_0} \rangle}{E_j - E} |\phi_j\rangle, \quad (\text{A5})$$

where E_j is the eigenvalue corresponds to the Bloch eigenfunction $|\phi_j\rangle$. This expansion is valid throughout the interior region A and on its surface (see Fig. 9).

To derive an equation for the R matrix, we now apply

this expansion of the scattering state on each boundary S_i . At each such boundary we can expand the scattering function in either lead eigenfunctions or Bloch eigenfunctions in the interior region. To be specific, we introduce a local Cartesian coordinate system for each lead: x_q and y_q are the longitudinal and transverse coordinates of the q^{th} lead, respectively. We choose $x_q = 0$ on each boundary. (One can easily choose any orthonormal coordinate system, *mutatis mutandis*). Each lead eigenfunction is then a product of a plane wave in the x_q direction and a transverse bound-state eigenfunction $\chi_n(y_q)$. The scattering wave function in the q^{th} lead therefore becomes

$$\begin{aligned} \Psi_{E,n_0}(x_p, y_p) &= e^{-ik_0 n_0 x_0} \chi_{0,n_0}(y_0) \delta_{p,0} \\ &+ \sum_{q,n_q=1}^N \tau_{q,n_q}(E) e^{ik_q n_q x_q} \chi_{q,n_q}(y_q) \delta_{p,q}, \end{aligned} \quad (\text{A6})$$

where k_{q,n_q} and τ_{q,n_q} are the wave vector and transmission *amplitude* for the channel with quantum number n_q in channel q . Also, $\chi_{n_q}(y_q)$ is the n_q^{th} transverse eigenfunction of lead q . Finally, $\delta_{p,q}$ is the Kroniker delta-function, which ensures that each wave function is defined only in one lead. If we measure energy in units of

E_0 then we can express energy conservation in lead q as $E = k_{q,n_q}^2 + n_q^2 \pi^2 / w_q^2$, where w_q is the width of the q^{th} lead (in units of w_0). We use this equation to determine the wave vector k_{q,n_q} .

After some algebra we get a set of linear algebraic equations that we can solve for the transmission amplitudes:

$$\begin{aligned} i \sum_{p,n_p} \tau_{p,n_p}(E) k_{p,n_p} M_{q,n_q,p,n_p}(E) - \tau_{q,n_q}(E) \\ = \delta_{q,0} \delta_{n_q,n_0} + ik_{0,n_0} M_{q,n_q,0,n_0}. \end{aligned} \quad (\text{A7})$$

In writing these equations we have defined

$$M_{q,n_q,p,n_p} = \int_{y_p} \int_{y_q} \chi_{q,n_q}^*(y_q) R_E(y_q, y_p) \chi_{p,n_p}(y_p) dy_q dy_p. \quad (\text{A8})$$

Finally, the R-matrix is given by

$$R(E, y_p, y_q) \equiv \sum_j \frac{\phi_j^*(x_q = 0, y_q) \phi_j(x_p = 0, y_p)}{E_j - E}. \quad (\text{A9})$$

This equation is general in that we can easily adapt it to any number of leads and to different choices of input lead.

- * Electronic address: morrison@mail.nhn.ou.edu
- ¹ *Thermodynamics and an Introduction to Thermostatistics*, Herbert. H. Callen, (John Wiley and Sons, 1985).
 - ² L. G. C. Rego, and G. Kirczenow, *Appl. Phys. Lett.*, **75**, 2262 (1999).
 - ³ Thushari Jayasekera, K. Mullen and Michael A. Morrison, *unpublished*.
 - ⁴ Junren Shi and X. C. Xie, *Phys. Rev. Lett.* **88**, 86401 (2002).
 - ⁵ W. Ketterle and N.J. van Druten, in *Advances in Atomic Molecular and Optical Physics*, **37**, B. Bederson and H. Walther eds. (Academic Press, San Diego, 1996), p181.
 - ⁶ R. Landauer, *Phil. Mag.* **21**, 863, (1970).
 - ⁷ M. Büttiker, *Phys. Rev. Lett.* **57** 1761 (1986).
 - ⁸ A. Douglas Stone and A. Szafer, *IBM J. Res. Dev.*, **32**, 384, (1988).
 - ⁹ E. P. Wigner and I. Eisenbud, *Phys. Rev.* **72**, 29 (1947).
 - ¹⁰ C. Bloch, *Nucl. Phys.* **4**, 503 (1957).
 - ¹¹ U. Wulf, J. Kucra, P. N. Racec and E. Sigmund, *Phys. Rev. B* **58** 16209, (1998).
 - ¹² Thushari Jayasekera, K. Mullen and Michael A. Morrison, "R-Matrix Theory in Confined Geometries," University of Oklahoma Ph.D thesis.
 - ¹³ R. Hilsch, *Rev. Sci. Inst.* **18**, 108 (1947).
 - ¹⁴ *And yet it moves: strange systems and subtle questions in physics*, M. P. Silverman, (Cambridge University Press, 1993).